Disentangling vertical land motion and waves from coastal sea level altimetry and tide gauges

Solène Dealbera, Rafael Almar, Fabrice Papa, Melanie Becker, Guy Wöppelmann

This paper presents a novel and global study regarding the contributions of the various components of relative sea level (RSL) at 434 sites worldwide, including Vertical Land Motion (VLM) and waves. For this, we combine concurrent observations from satellite altimetry, tide gauges and model hindcast in order to identify the predominant processes and drivers responsible for long-term variability and trend of RSL at the coast. We show that the dominant driver of the RSL trend is the ocean components in 76% of the cases, VLM in 17% and waves in 7%. Interestingly, no significant trend in the wave setup was noted over the period considered at most of our coastal stations, except for the Western Coast of the United States, where wave setup contributes to a decrease in RSL. In some regions, we highlight that the variance of RSL is partly due to waves from local or distant storms. We find that while removing this residual wave signal in VLM estimates has little impact on long-term trends, this correction allows to reinforce the level of significance in trends.

Disentangling vertical land motion and waves from coastal sea level altimetry and tide gauges

Solène Dealbera[a,b,*], Rafael Almar[a], Fabrice Papa[a,c], Mélanie Becker[d], Guy Wöppelmann[d]

[a]*LEGOS UMR5566, CNRS/CNES/IRD/UPS, 31400, Toulouse, France*
[b]*Univ. de Pau et des Pays de l'Adour/E2S UPPA, SIAME-MIRA, EA4581, 64600 Anglet, France*
[c]*Universidade de Brasilia, Instituto de Geociencias, Brasilia, Brazil*
[d]*LIENSs UMLR 7266 CNRS, La Rochelle University, 17000, La Rochelle, France*

Abstract

In the context of global mean sea level rise, understanding the drivers of relative sea-level (RSL) at the coast is of major importance for coastal environments research and management. Since the 1990s, the combination of satellite altimetry observations with *in situ* tide gauge data has provided a better understanding of coastal sea level variability, but challenges remain to quantify the relative contributions of possible drivers (oceanic, vertical land motion (VLM), atmospheric and wave). Here, over the period 1993-2015, we combine concurrent observations from satellite altimetry, tide gauges, and oceanic model hindcast in order to identify the predominant drivers responsible for long-term variability of RSL at 434 coastal locations worldwide. We found that the dominant driver of the RSL trend is the ocean components in 76% of the cases, VLM in 17% and waves in 7%. Interestingly, no significant trend in the wave setup was noted over the period considered at most of our coastal stations. However, at some locations, we found significant correlations between the wave setup hindcasts and VLM data. Moreover, we evidence a substantial variance reduction in the VLM once corrected for the wave setup. We therefore recommend future studies aiming at VLM estimation to consider applying wave setup corrections to improve the comparability of the tide gauge and satellite altimetry measurements.

Keywords: Sea level, Vertical land motion, Waves, Tide gauge, Satellite altimetry

1. Introduction

In the context of the current climate change, the impact of sea level rise on low-lying coastal zones (<10m elevation) is one of the major threats for more than 600 million people around the world (AR5, 2014; Neumann et al., 2015). Several studies have already shown the high degrees of vulnerability that many coastal areas and delta are facing, particularly in the intertropical zone, where highly populated regions and megacities, such as Mumbai, Bangkok, Jakarta or Lagos, are located (Nicholls et al., 2011; Hallegatte et al., 2013; Kulp and Strauss, 2019; Becker et al., 2019). Increased extreme sea levels will also exacerbate flood risk along the world coastlines if changes to coastal environments continue unmitigated (Oppenheimer et al., 2019; Almar et al., 2021). Sea level changes at the coast are subject to a combination of various physical processes, at different time scales, that originate in the ocean, the atmosphere and on land (Woodworth et al., 2019; Durand et al., 2019). In combination with tide gauge data, satellite radar altimetry data have underlined the complex sea level dynamics along the coasts, which can translate into differences in sea level change and variability

*Corresponding author: solene.dealbera@univ-pau.fr

between open ocean and coastal areas due to physical processes that interact with bathymetric and coastal properties (Woodworth et al., 2019). They have also underlined the current limitation of existing coastal sea level observing systems (Marcos et al., 2019), and the requirements for coastal hazards monitoring (Benveniste et al., 2019).

In particular, recent studies have suggested a contribution of wave setup to projected coastal sea level changes, more specifically an under-estimated wave contribution to coastal sea-level rise (Melet et al., 2018, 2020), which is not captured by altimetry (Gouzenes et al., 2020; Marti et al., 2019).

Examining the differences in satellite altimetry and tide gauge data has proven worthwhile for coastal studies in many respects in addition to stimulate the satellite altimetry community to revisit their data processing and validation schemes towards the coasts (Cipollini et al., 2017). Beyond the spatiotemporal sampling characteristics, it is important to remind that the two types of sea level measurements are different in essence. While satellite altimetry provides geocentric sea level information, i.e. with respect to the geocenter of a terrestrial reference frame, tide gauges record sea level with respect to the local solid earth surface upon which they are grounded (Gregory et al., 2019). The latter observed quantity thus contains vertical land motion (VLM) in addition to sea level information, which can be of paramount interest for coastal studies. For instance, land subsidence processes have been recognized as the dominant cause for permanent flooding and coastline retreat in the northern Gulf of Mexico, especially in the vicinity of New Orleans over the past decades (Allison et al., 2016). Recently, Becker et al. (2020) showed that when subsidence rates in the Ganges-Brahmaputra delta are considered, the IPCC sea level projections in the delta by 2100 could be double (under mitigate scenario). The changes in sea level relative to the land on which people live, is called the relative sea level (RSL).

Most of the studies investigating the differences in satellite altimetry and tide gauge data have concentrated on VLM signal. That is, the obvious difference from the above measurement quantity definitions. To the extent that both instruments measure identical ocean signals, their difference is a proxy for the vertical geocentric position of the tide gauge. Assuming that the environmental corrections and instrumental drifts are negligible, the time series of the sea level differences will then be dominated by VLM at the tide gauge. This approach with its assumptions was first published by Cazenave et al. (1999), and later on it has been refined in many subsequent studies (Wöppelmann and Marcos (2016) for a review; and references therein). This area of research still shows room for progress as can be noticed from the latest study published by Oelsmann et al. (2021).

In this study, we investigate whether there is evidence of a wave setup contribution in the satellite altimetry and tide gauge differences and try to estimate the contribution of wave to RSL variability and trends. We revisit to what extent the above-mentioned approach of VLM estimation and its assumptions hold, especially if there can be a bias in the current VLM estimates due to other possible drivers such as waves. To answer these questions, we used a climate and wave setup model hindcasts and we built upon the satellite altimetry and tide gauge data differences distributed by the Coastal Water Level Observing System (Système d'Observation du Niveau des Eaux Littorales, SONEL in french) portal (www.sonel.org) for 478 stations located along global coasts.

We firstly investigate the dominant drivers of sea level change at the coastal stations considered here, and propose global and regional maps highlighting the various contributions of these drivers. Interestingly, we will see that no significant trend in the wave setup is noted over the period considered at most of our coastal stations. However, significant correlations

between the wave setup hindcasts and the differences in satellite altimetry and tide gauge data are observed at some locations. As a result, no significant bias is introduced in the VLM estimates from these differences. Moreover, we evidence a substantial variance reduction in the differences once corrected for the wave setup. We therefore recommend future studies aiming at VLM estimation to consider applying wave setup corrections to improve the comparability of the tide gauge and satellite altimetry measurements. This will reduce the uncertainty and bring more confidence in the VLM estimates, but also avoid potential biases if the record length is short.

Section 2 firstly describes the various datasets used in the study and how the various information are combined. Section 3 presents the analysis and results while Section 4 builds on a discussion on a proposed wave correction and Section 5 deals with the conclusion.

2. Data

2.1. Tide gauge

The tide gauge (named hereafter t) monthly time series were retrieved from the Permanent Mean Sea Level Service (PSMSL) : www.psmsl.org (Holgate et al., 2013). The series affected by non-linear physical phenomena (e.g. earthquake, tsunami, large contribution from river discharges...) have been discarded for our study. A minimum time overlapping of 70% between altimetry data and t during the study period 1993-2015 allowed the selection of 478 tide gauge sites, mainly located in North America, Europe, Japan and Australia, but with sites available in South East Asia, the Indian and Pacific Ocean and South America.

2.2. Satellite altimetry

Sea level variations as seen from satellite altimetry observations (named hereafter a) include thermal and halosteric expansion, continental freshwater fluxes, i.e. ice sheets mass loss, mountain glaciers melting/growing and land water change, and mesoscale coastal circulation. These observations are available at various platforms: the service managing the Archiving, Validation and Interpretation of Satellite Oceanographic data (AVISO), the Climate Change Initiative (CCI), the Commonwealth Scientific and Industrial Research Organization (CSIRO), the Colorado University (CU) and the Goddard Space Flight Center (GSFC). On the basis of the results from Wöppelmann and Marcos (2016), who compared all these various altimetry-derived products together with tide gauges t, the AVISO product (spatial resolution of 1=4° and temporal resolution of 1 day) is used in the present study. The AVISO data are systematically corrected for Dynamical Atmospherical Correction (DAC, see 2.3, (Carrère and Lyard, 2003)) and geoid variations (Peltier, 1998). All a time series we consider in this study, which collocated to the tide gauge t, are also available at the SONEL website: www.sonel.org.

2.3. Dynamical Atmospheric Correction

There are several models to correct sea level from the atmospheric effects, the most known being the Inverted Barometer method, which is unfortunately incomplete because it only considers the static responses of the ocean to atmospheric pressure. Here we use a more advanced model, the Dynamical Atmospheric Correction (called hereafter d) as proposed by (Carrère and Lyard, 2003), which considers the dynamic response of the ocean to atmospheric forcing (pressure and wind). All tide gauge records were then corrected for d (Carrère and Lyard, 2003), as well as from the geoid variations due to the gravitational attraction of water mass redistribution (Peltier, 1998).

2.4. *Vertical land motion*

Following Wöppelmann and Marcos (2016), we estimate VLM using a combination of satellite altimetry and tide gauge data. The seasonally adjusted difference of the two series a and t allows to estimate VLM at 478 sites. In the following, VLM, noted vlm corresponds to t-a series and refers to changes in term of RSL.

2.5. *Waves setup*

Waves also plays an important role on coastal sea level variability and trend, as described in Melet et al. (2018). Waves have an oscillatory component called swash, and an average contribution called setup (named hereafter s). Here we consider only the wave setup and not the swash as swash has essentially an impact during extreme events with mainly an impact by overtopping and breaching of coastal protections. Wave setup is computed here from the commonly-used (Stockdon et al., 2006) generic empirical formulations:

$$s = 0.35\beta\sqrt{\frac{Hp}{Lp}} \quad (1)$$

In Eq. 1, coastal slope β is set constant to 0.1 (similarly to a global application in Melet et al. (2018)), Hp is the deep-water wave height, Lp is the deep-water peak wave wavelength and is related to the deep-water peak wave period Tp through the linear dispersion relationship $Lp = 1.56Tp^2$. For our analysis, only the time series of ERA-interim waves (Hp, Tp) nodes located within a radius of 0.5° around our selection of 478 tide gauge sites are kept. With this new criterion, the number of available sites for the analysis decreases from 478 to 434.

2.6. *Relative Sea Level and trend estimates*

RSL is a compound result of the combination of different drivers. Using the data described above, the long-term trend RSL can be decomposed as follows:

$$S_{RSL} = S_a + S_{vlm} + S_s + S_d \quad (2)$$

where a refers to the oceanic component derived from altimetry, vlm refers to vertical land motion, s refers to wave setup and d refers to the DAC (both pressure and wind friction effects). The term S (in mm/year) in Eq. 2 refers to the long-term trend of each component and is calculated using robust linear regression (Street et al., 1988). In the following, trends are considered statistically significant at p-value<0.1. For each site, the trend is estimated over the time periods intersected by all the series. Before trend estimations, all time series are deseasonalized, i.e. the seasonal signal is removed by subtracting the means for each month.

3. Analysis and Results

3.1. *Contributors to relative sea level rise*

Following Eq. 2, for each site, we first quantify the contribution of each component to RSL change at the coast. For a selected number of sites worldwide (for visual purpose not all sites are shown here), Fig. 1 shows the RSL trends along with the trend for each component.

The sample of sites enables to illustrate the large variety of resulting individual contributions to RSL.

Some sites clearly display a unique dominant factor, often vlm or a. As expected, trends in a are mainly positive for all the sites, while trends in vlm are found both positive (sinking land), such in Manila in Fig 1a, and negative (rising land) such as on the northwestern American coast (Fig 1b). Some sites display even contributions between vlm or a to RSL, such as on the eastern coast of the USA or in the Mediterranean sea, while sometimes opposite contributions between vlm or a seem to compensate each other, such as over the coat of Sweden (Fig 1c). Contributions of waves s are also at play for some regions, with negative contributions for instance in the Pacific Islands (Fig 1a) and positive on the eastern coast of Canada (Fig 1a).

The focus over the northwestern United States and western Canada (Fig. 1b), with an increased number of selected sites being displayed, confirms the dominant contribution of vertical land motion vlm in these regions mainly attributed to the Glacial Isostatic Adjustment (GIA) (Larsen et al., 2003; Mazzotti et al., 2008), caused by the melting of the polar ice caps approximately 20,000 years ago, whose effects is twofold, with an elastic adjustment of the Earth's crust modifying the altitude of the continents (10mm/year uplift at the poles, 5mm/year lowering at the Equator, Nicholls et al. (2021)) and a redistribution of water and mantle masses modifying the geoid. A more balanced contribution among the various components vlm, a and s arises along the western coast of the United States, with a contribution of waves at play.

Over northern Europe (Fig. 1c), positive trends in a are the dominant contributors in the North Sea, while negative trends in vlm compensate the positive trends in a in the Baltic Sea.

For all sites, Figure 2 shows which component is found to contribute the most to RSL trend over the 1993-2015 period. The dominant contributor for each site is estimated as the one having the maximum absolute trend within each component. Note that for all the studied sites, there is no maximum absolute trend which is not significant at 90%, thus all sites are circled in black. The box and whisker plots in Fig. 2 show the distribution of the significant trends for each component individually for all the sites. Note there is approximately an order of magnitude of 10 between the estimated trends for vlm and a as compared to s and d. While absolute values of trends can reach up to 10-20 mm/y for vlm and a, they are around 1-1.5 mm/y for s and d.

In Fig.1a, regional patterns are clearly depicted, with some large areas characterized by the dominant contribution of a single physical process. As suggested in Fig.1, in the Baltic Sea and in Alaska, the vertical land motion vlm trend dominates, following the well known GIA patterns. Local subsidence phenomena as the main contributor are also visible in the Gulf of Mexico, the Eastern Coast of the United States, Southern America, Southern Africa, Europe, Japan and around Manila, Philippines. For example, in Manila a noteworthy RSL of more than 10mm/y over 1993-2015 is confirmed with a dominant positive contribution of vertical land motion vlm, followed by a positive contribution of a, s, d in a smaller order of magnitude.

On the western coast of the United States, Canada, and around Hawaii, the dominance of wave component s trends is evidenced. Elsewhere, the oceanic component a clearly dominates as the largest contributing process to RSL. No site is dominated by the d component.

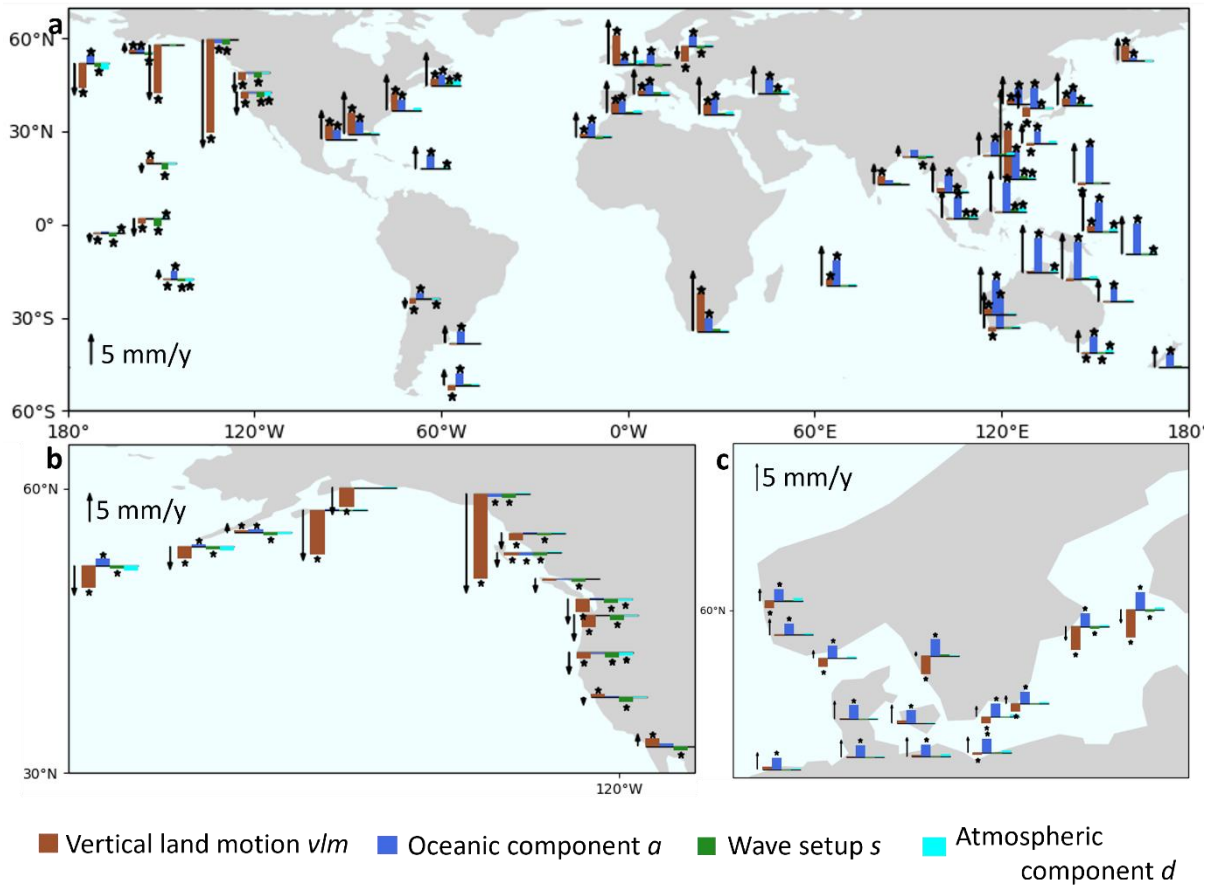

Figure 1: Contributions to long-term RSL trend over 1993 to 2015. a) Global map for a subset of 50 selected sites of RSL trend allocated among the different contributors: vertical land motion vlm (brown), oceanic component a (blue), wave s (green) and atmospheric component d (cyan). b) Regional map for the West coast of North America, c) Same as b) for North Sea and Baltic Sea in Europe. The RSL trend at each site (i.e. sum of all contributor trends) is indicated with an arrow, which length unit is given in mm/year. The star above the bar of a trend indicates its 90% significance.

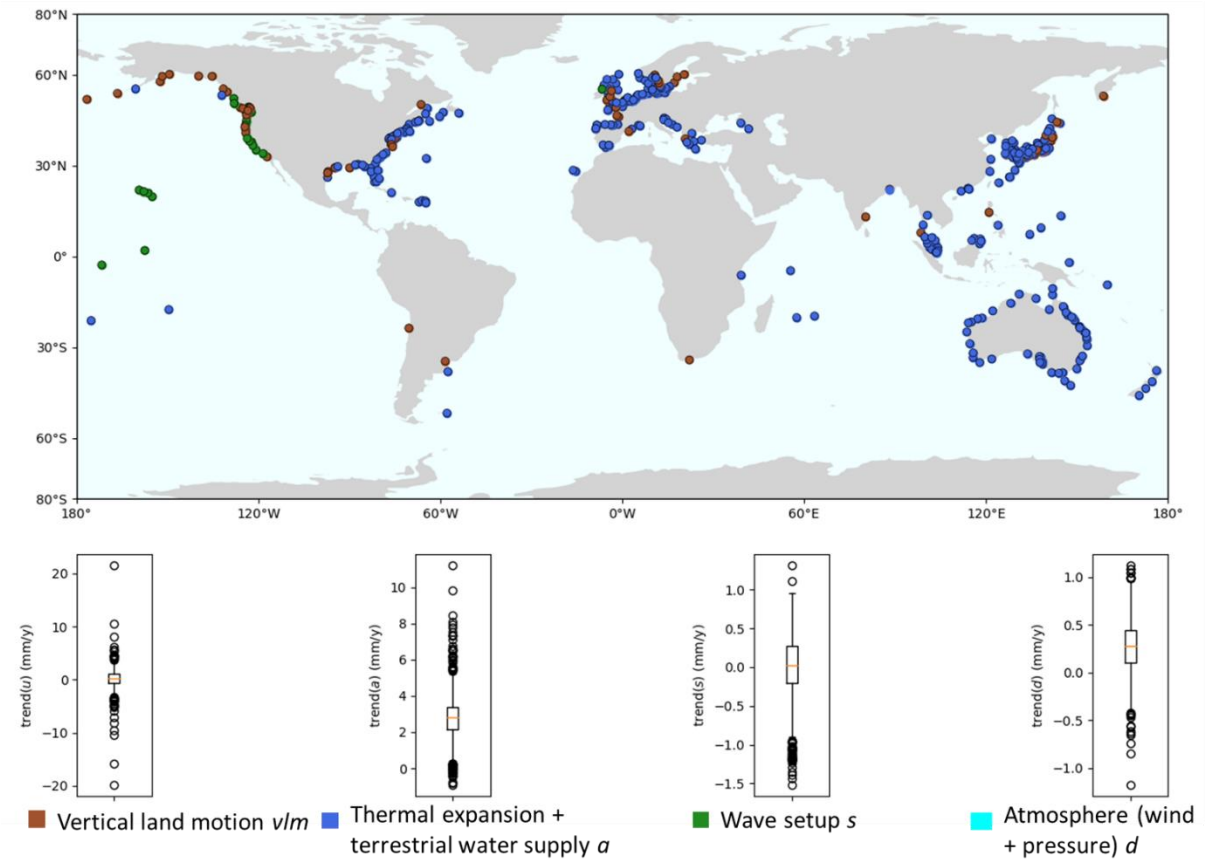

Figure 2: Global map of the dominant contribution to long-term RSL trend among : vertical land motion vlm (brown), oceanic component a (blue), wave s (green) and atmospheric component d (cyan). The dominant contributor corresponds to the component with the maximum absolute trend at each sites. The circles circled in black correspond to the 90% signifcant maximums. The boxplots of the trends for each component are shown in the lower panel.

A large majority of sites, 76% have a RSL trend dominated by the oceanic component a, while 17% are dominated by the vertical land motion vlm and only 7% by the wave contribution s.

3.2. Waves in vertical land motion time series

Although the preceding results show that the wave component s contributes in a lesser extend to RSL trend, as compared to a and vlm, questions still remain about its contribution to the overall RSL variability. This characterization remains indeed essential for an accurate assessment of RSL (Marti et al., 2019; Gouzenes et al., 2020).

Here we further propose to assess whether or not tide gauges record the long-term contribution of wave setup to sea level at the coast, significantly altering the long-term trends in RSL and in which case a correction could be applied to take into account this contribution. The question does not apply for the a series, since they represent process off the coast, where the setup phenomenon has no effect. The effects of the d were cautiously verified and corrected in s or vlm.

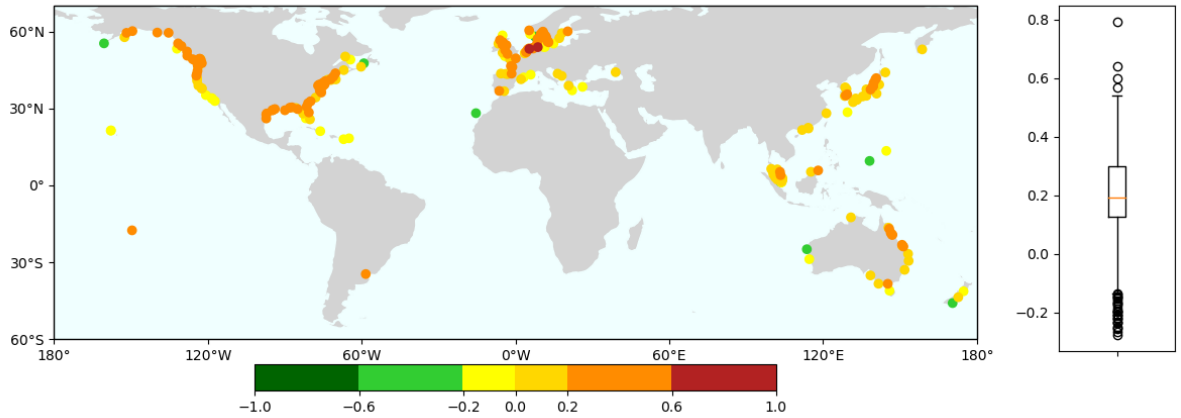

Figure 3: Global map of correlation coefficient and associated boxplot between wave s_t and vertical land motion vlm_t. Only sites with significant correlation higher than 90% are displayed.

Figure 3 shows the correlation between s_t and vlm_t (before estimating the correlation, both vlm and s time series are detrended and noted vlm_t and s_t respectively). On average, the correlation value are moderate around 0.2, with a maximum correlation of 0.79 recorded at the site Cuxhaven 2 station in Germany. Correlation coefficients larger than 0.2 emerge along the coasts of eastern and western Northern America and the coasts of northern Europe (Atlantic, Baltic and North Sea), while smaller secondary patterns are seen in Japan and the eastern coast of Australia. Those patterns are likely linked to storm tracks (eastern Northern America, northern Europe and Japan) and to the remote shores affected by the swells generated by those storms (western Northern America and Gulf of Mexico; Hoeke et al. (2013); Woodworth et al. (2019)).

Figure 4 shows the percentage vlm_t variance explained by the wave component s_t.

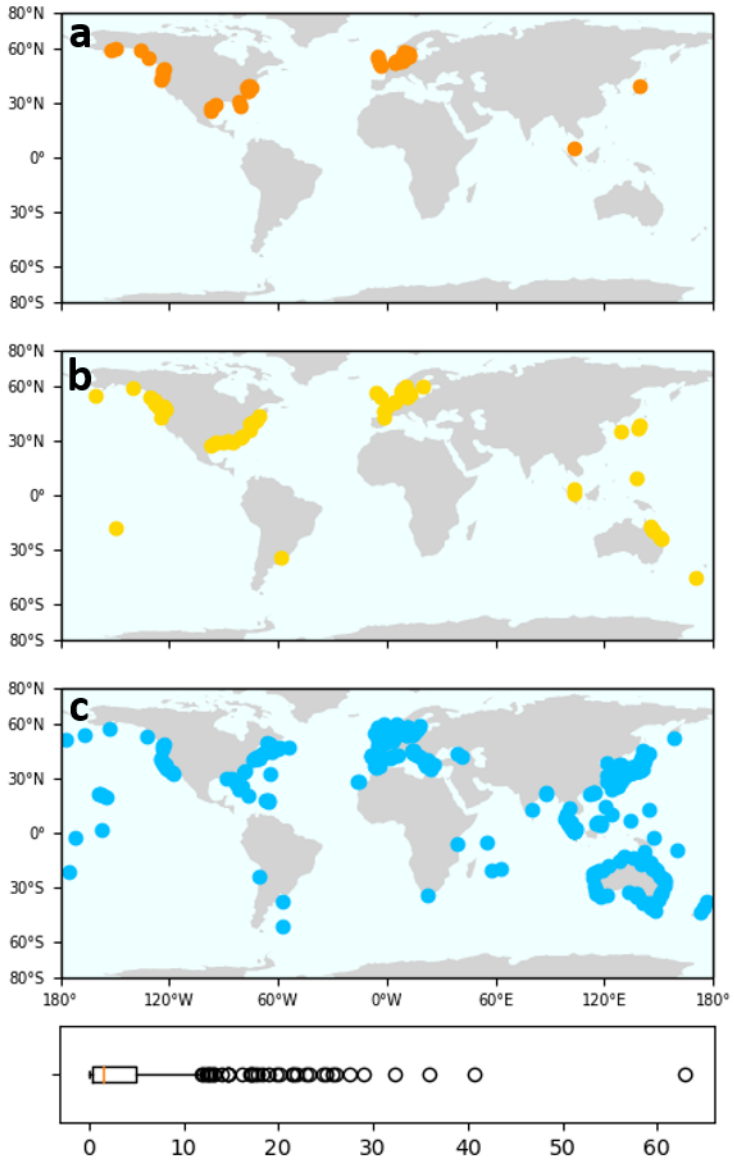

Figure 4: Map of the percentage of vlm_t variance explained by s_t : a) more than 11% (in orange), b) between 5 and 11% (in yellow), c) less than 5% (in blue). Only sites with a correlation between s_t and vlm_t significant at 90% are displayed. The boxplot represents the dispersion of the percentages.

The boxplots in Figure 4 show that the percentages of explained variance are generally small, and essentially between 0 and 10%, of which about half are between 0 and 5% with a median of 2%. Nevertheless, some sites show larger ratios with values ranging from 10 to more than 60%. To highlight the regional patterns, we classified the percentages in 3 groups (>11%, between 5% and 11% and <5%), the 11% threshold being taken as the upper whiskers (corresponding to highest percentage excluding outliers). The regional patterns observed in the correlation map in Figure 3 show that the largest contributions of the variability of waves s_t to vlm_t emerges on the West and East coasts of the United States and Canada, the North Sea and the Baltic Sea (Fig. 4a) with some contributions ranging between 20 and 40%.

The maximum contribution to the variability is found in Cuxhaven 2 station in Germany where the percentage of explained variance by s_t is 62%. This case also highlights the fact that it is not because s contributes to the sea level variability that it contributes to its trend. For this station, only a shows a significant trend at 90% (2.54*±1.00 mm/year) while the vlm and

s trends are small and non significant (0.44±0.61 mm/year and -0.08±0.32 mm/year respectively).

Nevertheless, on the Western Coast of North America, even if ~5% variance in vlm is explained by s, the contribution of s in the RSL is negligible with respect to the GIA dominated land motions. The trend of s is relatively constant along this stretch of coast, while the variance varies between 3% in the South and 9% in the North. One will even note the predominant impact of the oceanic factor in the Baltic Sea, compensated by the GIA along the coasts of Sweden and Finland. On the contrary, the contributions of vertical land movements and waves outweigh the oceanic contributions for the west coast of the United States and Canada. The regional patterns of trends are therefore unrelated to the patterns of variability of the s. This is because the contribution of the variance of s in vlm depends on the local tide gauge configuration, not only on wave variability.

4. Discussion on a wave correction for vertical land motion time series

As seen in the previous sections, no significant trend in the wave setup is noted over the period considered at most of the coastal stations. However, significant correlations are found between the wave setup and the VLM data.

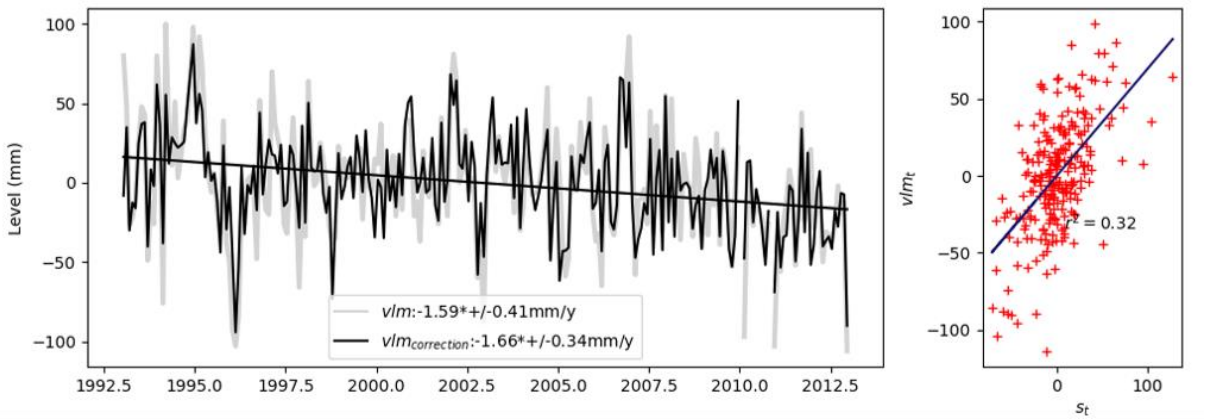

Figure 5: a) Time series and linear regression trend (mm/y) for vlm (light grey) and $vlm_{correction}$ (black) for the tide gauge Hirtshals located in Denmark. b) scatterplot between s_t and vlm_t with the linear regression between both estimates (back line) and the coefficient of determination r^2.

For the sites identified in Figure 4.a where the percentage of vlm variance explained by s is the largest, one can expect that taking into account the s effect might have a significant impact on the vlm signal. As previously seen, these locations can be influenced by mid-to high latitude storms but also by tropical cyclones, such as in the Gulf of Mexico. The impact of such events can be local but also generates energetic waves propagating over long distances which finally reach distant coasts with a potential influence on coastal sea level. Therefore, we propose to investigate a corrected time series of vlm, named $vlm_{correction}$, accounting for these contributions based on a linear regression.

As an illustration, Figure 5 shows a case study with the Hirtshals station (57.59N;9.97E), located in Denmark in the storm track areas of the North Sea and where s_t variability contributes substantially to vlm_t time series (Figure 4). The variance explained in vlm_t by the wave component s_t is shown in Figure 5b. Figure 5a clearly shows a substantial reduction in the variability of the time series between vlm and $vlm_{correction}$ when wave contribution is corrected. This also results in a slight change in the estimated trend (significant at 90%) from -1.59mm/y for vlm to -1.66mm/y $vlm_{correction}$, representing a change of 4.4%. Moreover, the

correction applied provides also lower standard errors (i.e. lower uncertainties) in the trend estimations, from +/- 0.41mm/y for vlm to +/-0.34mm/y for $vlm_{correction}$ or a change of 17%.

This case study clearly evidences a substantial variance reduction in VLM once corrected from the wave contribution, allowing to estimate a corrected VLM trend with reduced uncertainty and higher level of significance. Consequently, we investigate a similar procedure of correction for all the sites identified in Figure 4.a located in northern America and Europe.

The percentage changes in the $vlm_{correction}$ trend relative to the vlm trend and the associated standard errors are shown in Figure 6. Only sites with 90% significant trends are displayed. The relative changes in trends are essentially between -5 and 5% but peak at -20% and higher in North Western America coasts and few sites in Europe and the Gulf of Mexico (6.a and 6.b and boxplots). Additionally, the relative changes in the associated standard errors of trend estimations are relatively high, with values generally between -5 and -10% in norther America and between -9 and -12% in Europe, with some extreme values higher than -15% found along the Eastern and Western coasts of North America and the North Sea and Baltic Sea.

These values are non negligible and we recommend that the correction of wave variability to vlm time series should be considered and applied in future studies.

Some limitations on our approach, especially regarding the wave setup, should nevertheless be discussed here. Wave setup can be predicted using different methodologies, such as direct numerical modeling with process-based local coastal models, meta-models, and empirical formulations (Dodet et al., 2011; Melet et al., 2020). As process-based coastal models cannot yet simulate wave setup at global scale, wave setup was computed here from empirical formulations applied to global wave hindcast (based on EraInterim) which might have its own limitations when interpreted at the local scale. We also considered offshore deep water waves, assumed to impinge perpendicularly on the coast. In our estimates, the influence of shelf bathymetry on waves (shoaling, refraction) was not accounted for, even if Serafin et al. (2019) estimated locally a decrease of 5-10% of extreme wave events when accounting for wave transformation. On the other hand, a variety of empirical formulae exist to estimate wave setup (Dodet et al., 2011; Melet et al., 2020). Wave setup used in this study are estimated from the empirical formulation by Stockdon et al. (2006), which in general exhibit only relatively small differences from process-based models during modest wave conditions. Nonetheless, Stockdon et al. (2006) formulation tends to underestimate setup during extremes (H.E. et al., 2020), which the impact might be considered when interpreting our results. Similarly, the foreshore slope is an essential parameter in the estimation of wave setup. Global coastal slopes generally range between 0.01 and 0.20 and can substantially evolve in space and time (Serafin et al. (2019)). Here, we chose a time and space constant coastal slope value, which is commonly used for regional to global scale analysis (Vousdoukas et al. (2018)) since no observations of coastal slopes is currently available worldwide. Lastly, nonlinear interactions between components of coastal sea level are unaccounted for in our wave setup estimates, although they can be substantial, e.g. during storms. For instance, storm surge results in wave setup of greater amplitude (Idier et al. (2019)). However, resolving interactions between the different contributors to coastal sea level is currently out of the reach of modeling capacities. All these limitations should be accounted when interpreting the results at local scale.

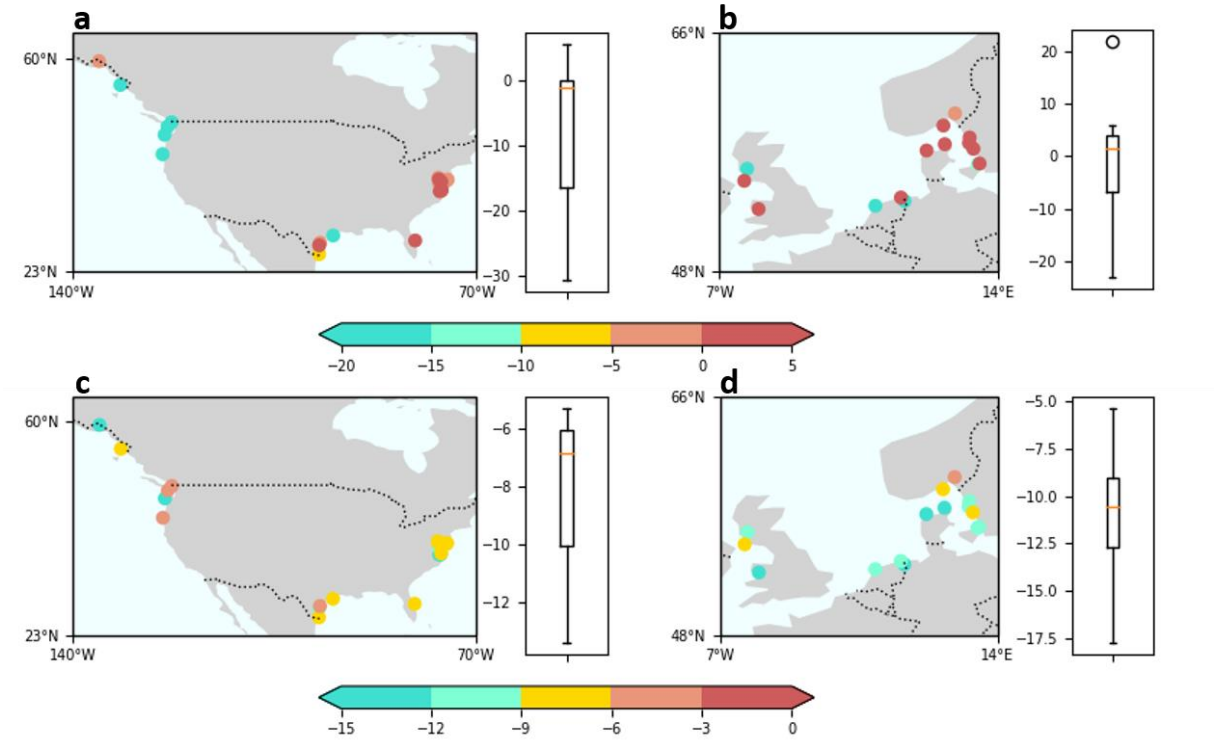

Figure 6: Map of the variation of trend($vlm_{correction}$) compared to trend(vlm) in %, for 90% significant trends, and associated box plots for North America (a) and northern Europe (b). Map of the variation of the standard error of trend($vlm_{correction}$) compared to the standard error of trend(vlm) in %, for 90% significant trends, and the associated boxplots for North America (c) and northern Europe (d).

5. Conclusions

In the last decades, satellite altimetry observations, in combination with *in situ* tide gauge data has enabled to progress towards a better understanding of coastal sea level variability at the coast, but challenges still remain to quantify the relative contributions of the possible drivers, especially vertical land motion (VLM) and wave (Benveniste et al. (2019); Melet et al. (2020)). Combining several observations accounting for the oceanic and atmospheric components, vertical land motion and wave, our study first investigates on the contributions of the various drivers of sea level change at the coast for 434 stations worldwide. We found that the dominant driver of the trend in RSL for 1993-2015 is the ocean components in 76% of the cases, VLM in 17% and waves in 7%. Regional increase in RSL is caused by the oceanic component, particularly on the western edges of the basins such as in the Pacific, and in Australia. VLM contributions are mainly located on the northwestern coast of America and the North and Baltic Seas in Europe, causing a decrease in RSL. Interestingly, at most of the coastal stations we studied, no significant trend in wave setup is revealed over the period considered and we found that wave setup contributes mainly to a decrease in RSL on the Western Coast of the United States. Nevertheless, despite the relatively small contribution of the wave to the trend at most of our coastal stations over the period considered, we reveal significant correlations between the wave setup hindcasts and the differences in satellite altimetry and tide gauge data. The largest significant correlation coefficients emerge along the coasts of eastern (Atlantic, Gulf of Mexico) and western (Pacific) Northern America and the coasts of northern Europe (Atlantic, Baltic and North Sea), while secondary patterns are observed in Japan and Australia. Those patterns corresponds to storm tracks locations and to the remote shores affected by the swells generated by those storm. In northern America and

Europe, we further analyze the relationship between VLM and waves and evidence a substantial variance reduction in VLM once we correct these time series from the wave setup contribution. Moreover, when estimating long term trends, it allows to reduce the uncertainty in the VLM trend estimates and reinforce their level of significance. Over those specific regions, our analysis therefore recommend future studies aiming at VLM estimation to consider applying wave setup corrections to improve the comparability of the tide gauge and satellite altimetry measurements.

Our study calls for further investigations to progress on our overall understanding of sea level changes at the coast, including the relative contributions of VLM and waves. For instance, satellite altimetry observations at the coast are constantly improving based on complete reprocessing of raw radar altimeter waveforms and future studies similar to the one we conducted should investigate newly sea level information available closer to the coast (Gouzenes et al. (2020); Marti et al. (2019)) as it may differs substantially from sea level away from the coast. Refined method for VLM determination (Oelsmann et al. (2021)) should also be considered. In addition, there are several methodologies to estimate wave setup and with future expected improvements on the characteristics of the parameters used (slopes, bathymetry, non linear interactions), finer studies on the contribution of waves at the coast to RSL will be possible in order to confirm our findings. Hindcasts estimates are constantly improving, in particular at the coasts, with better grid resolution and greater number of processes (e.g. the use of Era5 now) and should be used in similar analysis.

Regarding the contribution of other small-scale coastal processes to RSL, fresh water input from rivers could also be non negligible in some regions located to large freshwater outlets (Becker et al. (2020), Durand et al. (2019)), such as the Ganges-Brahmaputra, La Plata or the Mississippi rivers to name a few. The contribution of river ow to sea level variations recorded at the tide gauges and off shore should be also further investigated towards a more comprehensive understanding of relative sea level change at the coast.

Finally, the various criteria we considered (study period of 1993-2015, concurrent observations of the various 349 components, etc) allowed us to analyze a selection of 434 sites, mainly located in North America, Europe, Japan and Australia, with sites also available in South East Asia, the Indian and Pacific Ocean and South America. These sites already cover a wide range of environments, but a lack of tide gauge observations leaves many parts of the African and South American Atlantic coasts, a large part of eastern Pacific and the African coasts in the Indian ocean out of our analyzes. This obviously calls for the need to collect long term information about the coastal zones and their evolution in these regions, with obvious scientific and societal interests to understand the various drivers of sea level change at the coast.

References

Allison, M., Yuill, B., Törnqvist, T., Amelung, F., Dixon, T., Erkens, G., Stuurman, R., Jones, C., Milne, G., Steckler, M., Syvitski, J., Teatini, P., 2016. Global risks and research priorities for coastal subsidence. Eos Transactions American Geophysical Union 97, 22-27. doi:10.1029/2016EO055013.

Almar, R., Ranasinghe, R., Bergsma, E., Diaz, H., Melet, A., Papa, F., Vousdoukas, M., Athanasiou, P., Dada, O., Almeida, L.P., Kestenare, E., 2021. A global analysis of extreme coastal water levels with implications for potential coastal overtopping. Nature Communications 12, 3775. doi:10.1038/s41467-021-24008-9.

AR5, I., 2014. Climate Change 2014: Synthesis Report. Contribution of Working Groups I, II and III to the Fifth Assessment Report of the Intergovernmental Panel on Climate Change. Technical Report. IPCC, Geneva, Switzerland.

Becker, M., Karpytchev, M., Papa, F., 2019. Hotspots of relative sea level rise in the tropics. Tropical Extremes: Natural Variability and Trends, 203-262. doi:10.1016/B978-0-12-809248-4.00007-8.

Becker, M., Papa, F., Karpytchev, M., Delebecque, C., Krien, Y., Khan, J.U., Ballu, V., Durand, F., Cozannet, G.L., Islam, A.K.M.S., Calmant, S., Shum, C.K., 2020. Water level changes, subsidence, and sea level rise in the ganges-brahmaputra-meghna delta. PNAS 117, 1867-1876. doi:10.1073/pnas.1912921117.

Benveniste, J., Cazenave, A., Vignudelli, S., Fenoglio-Marc, L., Shah, R., Almar, R., Andersen, O., Birol, F., Bonnefond, P., Bouffard, J., Calafat, F., Cardellach, E., Cipollini, P., Le Cozannet, G., Dufau, C., Fernandes, M., Frappart, F., Garrison, J., Gommenginger, C., Han, G., Høyer, J., Kourafalou, V., Leuliette, E., Li, Z., Loisel, H., Madsen, K., Marcos, M., Melet, A., Meyssignac, B., Pascual, A., Passaro, M., Ribó, S., Scharroo, R., Song, Y., Speich, S., Wilkin, J., Woodworth, P., Wöppelmann, G., 2019. Requirements for a coastal hazards observing system. Frontiers in Marine Science 6. doi:10.3389/fmars.2019.00348.

Carrère, L., Lyard, F., 2003. Modeling the barotropic response of the global ocean to atmospheric wind and pressure forcing - comparisons with observations. Geophysical Research Letters 30, 1275. doi:10.1029/2002GL016473.

Cazenave, A., Dominh, K., Ponchaut, F., Soudarin, L., Cretaux, J.F., Le Provost, C., 1999. Sea level changes from topex-poseidon altimetry and tide gauges, and vertical crustal motions from doris. Geophysical Research Letters 26, 2077-2080. doi:10.1029/1999GL900472.

Cipollini, P., Benveniste, J., Birol, F., Fernandes, M., Passaro, M., Vignudelli, S., 2017. Satellite altimetry in coastal regions, in: Stammer, D., Cazenave, A. (Eds.), Satellite Altimetry Over Oceans and Land Surfaces Earth Observation of Global Changes Book Series. London: CRC Press, p. 644. doi:10.1201/9781315151779-11.

Dodet, G., Melet, A., Ardhuin, F., Bertin, X., Idier, D., Almar, R., 2011. The contribution of wind-generated waves to coastal sea-level changes. Surveys in Geophysics 40, 1563-1601. doi:10.1007/s10712-019-09557-5.

Durand, F., Piecuch, C.G., Becker, M., Papa, F., Raju, S.V., Khan, J.U., Ponte, R.M., 2019. Impact of continental freshwater runoff on coastal sea level. Surveys in Geophysics 40, 1437-1466. doi:10.1007/s10712-019-09536-w.

Gouzenes, Y., Léger, F., Cazenave, A., Birol, F., Bonnefond, P., Passaro, M., Nino, F., Almar, R., Laurain, O., Schwatke, C., Legeais, J.F., Benveniste, J., 2020. Coastal sea level rise at senetosa (corsica) during the jason altimetry missions. Ocean Science 16, 1165-1182. doi:10.5194/os-16-1165-2020.

Gregory, J.M., Griffies, S.M., Hughes, C.W., Lowe, J.A., Church, J.A., Fukumori, I., Gomez, N., Kopp, R.E., Landerer, F., Le Cozannet, G., Ponte, R.M., Stammer, D., Tamisiea, M.E., van de Wal, R.S.W., 2019. Correction to: Concepts and terminology for sea level: Mean, variability and change, both local and global. Surveys in Geophysics 40, 1291-1292. doi:10.1007/s10712-019-09555-7.

Hallegatte, S., Green, C., Nicholls, R., Corfee-Morlot, J., 2013. Future flood losses in major coastal cities. Nature Climate Change 3, 802-806. doi:10.1038/nclimate1979.

H.E., P., Gharabaghi, B., Bonakdari, H., Robertson, B., Atkinson, A., Baldock, T., 2020. Prediction of wave runup on beaches using gene-expression programming and empirical relationships. Coastal Engineering 144, 47-61.

Hoeke, R.K., McInnes, K.L., Kruger, J.C., McNaught, R.J., Hunter, J.R., Smithers, S.G., 2013. Widespread inundation of pacific islands triggered by distant source wind-waves. Global and Planetary Change 108, 128-138. URL: https://www.sciencedirect.com/science/article/pii/S0921818113001483, doi:https://doi.org/10.1016/j.gloplacha.2013.06.006.

Holgate, S.J., Matthews, A., Woodworth, P.L., Rickards, L.J., Tamisiea, M.E., Bradshaw, E., Foden, P.R., Gordon, K.M., Jevrejeva, S., Pugh, J., 2013. New Data Systems and Products at the Permanent Service for Mean Sea Level. Journal of Coastal Research 29, 493-504. doi:10.2112/JCOASTRES-D-12-00175.1.

Idier, D., Bertin, X., Thompson, P., Pickering, M., 2019. Interactions between mean sea level, tide, surge and flooding: Mechanisms and contributions to sea level variations at the coast. Surveys in Geophysics doi:10.1007/s10712-019-09549-5.

Kulp, S.A., Strauss, B.H., 2019. New elevation data triple estimates of global vulnerability to sea-level rise and coastal flooding. Nature Communications 10. doi:10.1038/s41467-019-12808-z.

Larsen, C.F., Echelmeyer, K.A., Freymueller, J.T., Motyka, R.J., 2003. Tide gauge records of uplift along the northern pacific-north american plate boundary, 1937 to 2001. Journal of Geophysical Research 108. doi:10.1029/2001JB001685.

Marcos, M., Wöppelmann, G., Matthews, A., Ponte, R.M., Birol, F., Ardhuin, F., Coco, G., Santamaría-Gómez, A., Ballu, V., Testut, L., Chambers, D., Stopa, J.E., 2019. Coastal sea level and related fields from existing observing systems. Surveys in Geophysics 40, 293-1317. doi:10.1007/s10712-019-09513-3.

Marti, F., Cazenave, A., Birol, F., Passaro, M., Léger, F., Niño, F., Almar, R., Benveniste, J., Legeais, J.F., 2019. Altimetry-based sea level trends along the coasts of western africa. Advances in Space Research doi:10.1016/j.asr.2019.05.033.

Mazzotti, S., Jones, C., , Thomson, R.E., 2008. Relative and absolute sea level rise in western canada and northwestern united states from a combined tide gauge-gps analysis. Journal of Geophysical Research 113. doi:10.1029/2008JC004835.

Melet, A., Almar, R., Hemer, M., Le Cozannet, G., Meyssignac, B., Ruggiero, P., 2020. Contribution of wave setup to projected coastal sea level changes. Journal of Geophysical Research: Oceans 125. doi:10.1029/2020JC016078.

Melet, A., Meyssignac, B., Almar, R., Le Cozannet, G., 2018. Under-estimated wave contribution to coastal sea-level rise. Nature Climate Change 8, 234{239. doi:10.1038/s41558-018-0088-y.

Melet, A., Teatini, P., Le Cozannet, G., Jamet, C., Conversi, A., Benveniste, J., Almar, R., 2020. Earth observations for monitoring marine coastal hazards and their drivers. Surveys in

Geophysics [Early access], p. [46 p.]. URL: http://www.documentation.ird.fr/hor/fdi:010078173, doi:10.1007/s10712-020-09594-5.

Neumann, B., Vafeidis, A.T., Zimmermann, J., Nicholls, R.J., 2015. Future coastal population growth and exposure to sea-level rise and coastal flooding - a global assessment. PLos ONE 10. doi:10.1371/journal.pone.0118571.

Nicholls, R.J., Lincke, D., Hinkel, J., Brown, S., Vafeidis, A.T., Meyssignac, B., Hanson, S.E., Merkens, J.L., Fang, J., 2021. A global analysis of subsidence, relative sea-level change and coastal flood exposure. Nature Climate Change doi:10.1038/s41558-021-00993-z.

Nicholls, R.J., Marinova, N., Lowe, J.A., Brown, S., Vellinga, P., de Gusmão, D., Hinkel, J., Tol, R.S.J., 2011. Sea-level rise and its possible impacts given a `beyond 4°c world` in the twenty-first century. Philosophical Transactions: Mathematical, Physical and Engineering Sciences 369, 161-181. doi:10.2307/25759992.

Oelsmann, J., Passaro, M., Dettmering, D., Schwatke, C., Sánchez, L., Seitz, F., 2021. The zone of influence: matching sea level variability from coastal altimetry and tide gauges for vertical land motion estimation. Ocean Science 17, 35-57. doi:10.5194/os-17-35-2021.

Oppenheimer, M., Glavovic, B., Hinkel, J., R. van de Wal, A.M., Abd-Elgawad, A., Cai, R., Cifuentes-Jara, M., DeConto, R., Ghosh, T., Hay, J., Isla, F., Marzeion, B., Meyssignac, B., Sebesvari, Z., 2019. Sea level rise and implications for low lying islands, coasts and communities, in: Pörtner, H.O., Roberts, D., Masson-Delmotte, V., Zhai, P., Tignor, M., Poloczanska, E., Mintenbeck, K., Alegría, A., Nicolai, M., Okem, A., Petzold, J., Rama, B., Weyer, N. (Eds.), IPCC Special Report on the Ocean and Cryosphere in a Changing Climate. IPCC. chapter 4, p. 169.

Peltier, W.R., 1998. Postglacial variations in the level of the sea: Implications for climate dynamics and solid-earth geophysics. Reviews of Geophysics 36, 603-689.

Serafin, K., Ruggiero, P., Barnard, P., Stockdon, H., 2019. The influence of shelf bathymetry and beach topography on extreme total water levels: Linking large-scale changes of the wave climate to local coastal hazards. Coastal Engineering 150, 1-17.

Stockdon, H.F., Holman, R.A., Howd, P.A., Sallenger Jr, A.H., 2006. Empirical parameterization of setup, swash, and runup. Coastal Engineering 53, 573-588.

Street, J.O., Carroll, R.J., Ruppert, D., 1988. A note on computing robust regression estimates via iteratively reweighted least squares. The American Statistician 42, 152-154. doi:10.2307/2684491.

Vousdoukas, M., Mentaschi, L., Voukouvalas, E., Verlaan, M., Jevrejeva, S., Jackson, L., Feyen, L., 2018. Global probabilistic projections of extreme sea levels show intensification of coastal flood hazard. Nature Communications 9(144), 2360.

Woodworth, P.L., Melet, A., Marcos, M., Ray, R.D., Wöppelmann, G., Sasaki, Y.N., Cirano, M., Hibbert, A., Huthnance, J.M., Monserrat, S., Merrifield, M.A., 2019. Forcing factors affecting sea level changes at the coast. Surveys in Geophysics 40, 1351-1397. doi:10.1007/s10712-019-09531-1.

Wöppelmann, G., Marcos, M., 2016. Vertical land motion as a key to understanding sea level change and variability. Reviews of Geophysics 54, 64-92. doi:10.1002/2015RG000502.